Green fluorescent protein-based halide indicators with improved chloride and iodide affinities

Luis J.V. Galietta[1], Peter M. Haggie[1], A.S. Verkman*

Departments of Medicine and Physiology, Cardiovascular Research Institute, 1246 Health Sciences East Tower, University of California, San Francisco, CA 94143-0521, USA

Received 11 April 2001; revised 22 May 2001; accepted 23 May 2001

First published online 6 June 2001

Edited by Matti Saraste

Abstract The green fluorescent protein YFP-H148Q is sensitive to halides by a mechanism involving halide binding and a shift in pK_a. However, a limitation of YFP-H148Q is its low halide sensitivity, with $K_d > 100$ mM for Cl^-. Indicators with improved sensitivities are needed for cell transport studies, particularly in drug discovery by high-throughput screening, and for measurement of Cl^- concentration in subcellular organelles. YFP-H148Q libraries were generated in which pairs of residues in the vicinity of the halide binding site were randomly mutated. An automated procedure was developed to screen bacterial colonies for improved halide sensitivity. Analysis of 1536 clones revealed improved anion sensitivities with K_d down to 2 mM for I^- (I152L), 40 mM for Cl^- (V163S), and 10 mM for NO_3^- (I152L). The anion-sensitive mechanism of these indicators was established and their utility in cells was demonstrated using transfected cells expressing the cystic fibrosis transmembrane conductance regulator chloride channel.

Key words: Green fluorescent protein; Chloride channel; Cystic fibrosis; High-throughput

1. Introduction

Chloride is the major anion in cellular compartments. The measurement of chloride transport is important in defining mechanisms of fluid secretion, neurosynaptic transmission, and cell volume regulation. Our laboratory has developed a series of halide-sensitive chemical fluorescent indicators of the quinolinium [1] and pyrido[2,1-h]-pteridin [2] classes. However, fundamental limitations of chemical-type indicators for cellular applications are the need for cell loading and washing, imperfect indicator retention in cells, and the inability to target the indicator to specified subcellular locations.

Based on the halide binding properties of yellow fluorescent variants (YFP) of the green fluorescent protein (GFP) [3], we recently reported the halide sensitivity mechanism and cellular applications of mutant YFP-H148Q [4]. YFP-H148Q fluorescence is pH-sensitive, with a pK_a of 7.1 in the absence of Cl^- which increases by 0.7 pH units at 400 mM Cl^-. At a constant pH of 7.5, YFP-H148Q fluorescence decreases ~2-fold with increasing Cl^- with a K_d of 100 mM, and by up to 85% with increasing I^- with a K_d of 21 mM. Biophysical measurements suggested a unique halide binding site in the YFP molecule distinct from but near to its triamino acid chromophore [4]. Recently, the crystal structure of the YFP-H148Q/I^- complex was solved, revealing at least 10 residues in the vicinity of the I^- binding site [5].

The low sensitivity of YFP-H148Q fluorescence to Cl^- is a significant limitation in its application to measurements of cellular Cl^- concentration and transport. Because of the interior negative cell membrane potential cytoplasmic [Cl^-] is generally less than 40 mM, and although no information is available, [Cl^-] is not likely to be much higher in organelles of the endosomal and secretory compartments. Although I^- can be substituted for Cl^- in some transport measurements, the moderate sensitivity of YFP-H148Q fluorescence to I^- requires substantial concentrations of I^- (~100 mM) to produce acceptable signal changes. Iodide is not a native cellular constituent and at high concentrations can inhibit transport processes and manifest cell toxicity. Exchange of NO_3^- for Cl^- is a preferred approach to measure cystic fibrosis transmembrane conductance regulator (CFTR)-mediated halide transport; however, the sensitivities of YFP-H148Q to Cl^- and NO_3^- are comparable and low. The purpose of this study was to identify YFP mutants with improved properties compared to YFP-H148Q. By screening a targeted set of YFP mutants, we discovered mutants with substantially improved Cl^-, I^-, and NO_3^- sensitivities, including a mutant in which the K_d for Cl^- was lower than that for I^- and another in which Cl^- and NO_3^- sensitivities were sufficiently different to permit transport measurements using NO_3^-/Cl^- exchange. The YFP mutants were characterized and their application to measurements in living cells was demonstrated.

2. Materials and methods

2.1. cDNA expression libraries for random site-specific YFP mutagenesis

Mutagenesis was performed using the polymerase chain reaction-based QuickChange™ Site-Directed mutagenesis kit (Stratagene). Plasmid pEYFP encoding the enhanced YFP (EYFP = GFP-S65G/V68L/S72A/T203Y, Clontech) [6] was used as template. The mutation H148Q was introduced in the coding region of pEYFP to generate plasmid pEYFP-H148Q for use as template for engineered and random mutagenesis. Three mutational libraries were generated in which

*Corresponding author. Fax: (1)-415-665 3847; http://www.ucsf.edu/verklab. E-mail: verkman@itsa.ucsf.edu

[1] These authors contributed equally.

Abbreviations: G/YFP, green/yellow fluorescent protein; CFTR, cystic fibrosis transmembrane conductance regulator

PII: S0014-5793(01)02561-3

residues at positions 150 and 152, 161 and 163, and 201 and 203 were randomly mutated. Using pEYFP-H148Q as template, 52-mer primers were designed to randomly mutate amino acids in pairs by introducing random codons (NNN) at specified locations.

2.2. Screening of YFP mutants

The mutational libraries were transformed into JM109 *Escherichia coli* (Promega) and plated on LB plates supplemented with 50 μg/ml ampicillin and 1 mM IPTG. Plates were incubated at 37°C for 24 h followed by a further 24 h at 4°C. Colony density was 200–300 per plate. Individual fluorescent bacterial colonies were identified using ultraviolet illumination and transferred to 96-well microplates containing 200 μl per well of LB medium supplemented with 50 μg/ml ampicillin and 1 mM IPTG. In addition to selecting visibly fluorescent colonies, 200–300 additional colonies from the libraries were chosen. Bacteria in 96-well plates were incubated overnight at 37°C in a shaker incubator. Replicate microplates and LB/agar plates were generated using a microplate replicator (Fisher).

Bacteria in 96-well master plates were lysed in situ by incubation (30 min, 4°C) with 20 μl of 10 mg/ml lysozyme in 25 mM HEPES, 25 mM MES (pH 7.5) and three freeze-thaw cycles. 10 μl of lysate per well was then transferred to 96-well plates containing 170 μl of 25 mM HEPES, 25 mM MES (pH 7.5). Halide sensitivities of YFP mutants were determined automatically using a FLUOstar Galaxy microplate reader (BMG LabTechnologies, Inc.) equipped with HQ500/20X (500 ± 10 nm) excitation and HQ535/30M (535 ± 15 nm) emission filters (Chroma Technology Corp.) and syringe pumps. Additions of NaCl or NaI (0.5 M or 1 M stocks in 25 mM HEPES, 25 mM MES, pH 7.5) were done to titrate halide concentrations from 0 to 200 mM for K_d determination.

2.3. Purification of recombinant YFP mutants

Coding regions of selected YFP mutants were subcloned into plasmid pRSET B, which contains a 6-histidine N-terminal tag (Invitrogen), at *Bam*HI/*Eco*RI sites. *E. coli* BL21(DE3) cells were transformed, plated onto LB plates containing 100 μg/ml ampicillin, cultured for 24 h at 37°C, and stored for 48 h at 4°C. Proteins were purified to homogeneity (judged by gel electrophoresis) using Ni-NTA agarose resin (Qiagen) according to the manufacturer's instructions, except that NaCl was replaced by Na gluconate in all buffers. Following purification, buffer exchanges were done using Centricon Plus20 ultrafiltration units with 10 000 molecular size cut-off (Amicon).

2.4. Determination of halide sensitivities and pK_a

Solutions of purified YFP mutant proteins were measured in the BMG plate reader to determine halide affinities and pK_a. Anion titrations were performed in triplicate in 50 mM Na phosphate buffer (pH 7.35) containing 400 mM total concentrations of Na gluconate and the Na salt of the anion of interest. Dissociation constants (K_d) were determined from fluorescence (F) titrations using the equation $F = a[X^-]/(K_d+[X^-])+b$, where $[X^-]$ is halide concentration and $1-b/a$ is the fractional decrease in fluorescence at high $[X^-]$. pH titrations were performed in triplicate in 25 mM MES, 25 mM HEPES, 150 mM Na Cl^-/gluconate buffers in the pH range 5–10. The pK_a was determined using the equation $F = A+B[1+10^{(pK_a-pH)nH}]^{-1}$, where n_H is the Hill coefficient.

2.5. Spectroscopic and kinetic measurements

Absorbance measurements were performed on a Hewlett-Packard 8452 diode array spectrophotometer. Fluorescence spectra were obtained using a Fluorolog spectrofluorimeter (Spex Industries). Fluorescence lifetimes were determined using an SLM 48000 MHF fluorimeter by multi-frequency phase-modulation fluorimetry (488 nm excitation, > 520 nm emission) using fluorescein in 0.1 N NaOH as reference (lifetime 4.0 ns). Molar extinction coefficients and quantum yields were determined relative to YFP using the standardized conditions of Cubitt et al. [7] at pH 8.0 in 10 mM Tris, 10 mM EDTA. Proteins were centrifuged (100 000 × g for 30 min) prior to determinations and it was assumed that the YFPs were pure and fully matured. Protein concentrations for computation of molar extinction coefficients were determined using the Bio-Rad Protein Assay Reagent with bovine serum albumin as standard. Kinetic measurements of YFP–Cl^- association and dissociation were done on a Hi-Tech SF51 stopped-flow apparatus using 500 ± 10 nm excitation filter and 530 nm long-pass emission filter. The time course of mutant YFP fluorescence (in 50 mM Na phosphate buffer, pH 7.35) was measured in response to rapid changes in solution $[Cl^-]$ from 0 to 40 mM and from 40 to 20 mM.

2.6. Cell measurements

The coding sequences of selected mutant YFPs were subcloned into mammalian expression plasmid pcDNA3.1 (Invitrogen). Swiss 3T3 fibroblasts expressing wild-type human CFTR were plated on coverglasses (18 mm diameter) and transfected with 1 μg of plasmid using Lipofectamine™ (Gibco BRL) according to the manufacturer's instructions. Cells were grown at 37°C (95% air, 5% CO_2) using DME H-21 medium. After 24–48 h, the coverglasses were mounted in a custom built low-volume cell chamber for perfusion at 8–10 ml/min at 37°C. Cell fluorescence was measured continuously on an inverted epifluorescence microscope (Nikon Diaphot) using a dry objective (Leitz, 25×, NA 0.35), filter cube (500 ± 10 nm excitation, 535 ± 15 emission, 515 nm dichroic (Chroma)) and photomultiplier detector. Cl^-/I^- and Cl^-/NO_3^- exchange protocols were performed by switching the perfusate between phosphate-buffered saline (137 mM NaCl, 2.7 mM KCl, 0.7 mM $CaCl_2$, 1.1 mM $MgCl_2$, 1.5 mM KH_2PO_4, 8.1 mM Na_2HPO_4, pH 7.4) and solutions in which specified amounts of NaCl were replaced by NaI or $NaNO_3$.

3. Results

Random mutations were introduced in the six hydrophobic residues lining the YFP-H148Q halide binding site in an attempt to modify the polarity and/or size of the cavity and thus halide binding affinities. We used degenerate primers to produce YFP-H148Q libraries containing mutations in residue pairs valine 150 and isoleucine 152, valine 163 and phenylalanine 165, and leucine 201 and tyrosine 203. After growth on IPTG agar plates, approximately 20% and 40% of colonies were fluorescent for the Val150/Ile152 and Val163/Phe165

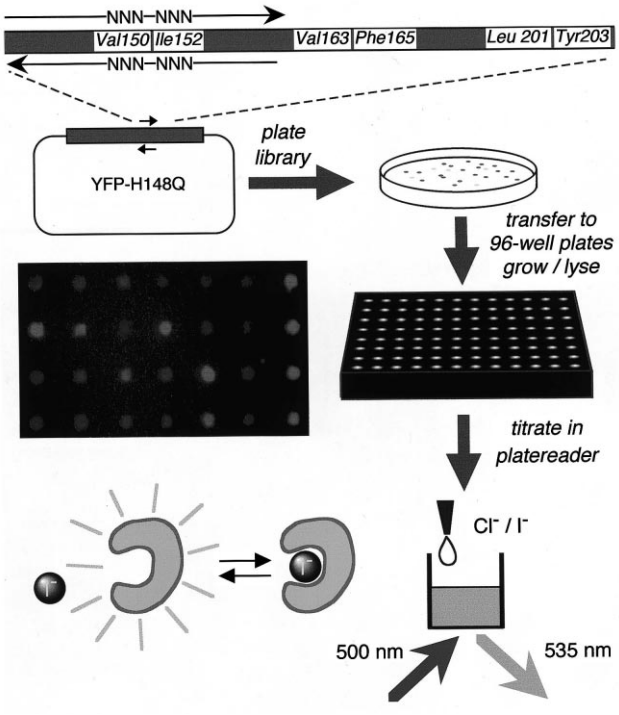

Fig. 1. Strategy for generating and screening of YFP mutational libraries. Indicated pairs of amino acids were randomly mutated using appropriate primers. Transformed bacterial colonies were transferred to 96-well microplates for growth, lysis and titration. See Section 2 for details. Inset: photograph of a section of a plate showing arrayed bacterial colonies with differing amounts of fluorescence.

Table 1
Halide sensitivities of YFP mutants

Mutant	K_{Cl} (mM)[a]	K_I (mM)
No mutation	197	20
I152L	88	3
V150A/I152L	61	9
V150T	262	11
I152Y	132	13
V163G	136	72
V163S	62	107
V163T	124	21
V163L	77	21
V163N	107	6
V163A/F165Y	168	15
V163T/F165Y	55	5
V150Q/V163S	190	115
V150S/V163S	169	149
V150S/V163T	92	117
V150T/V163Q	288	127
V150T/V163S	253	152

[a]Cl^- and I^- affinities (K_{Cl} and K_I) were measured in 96-well microplates at pH 7.5 as described in Section 2. Each well contained a bacterial lysate with YFP-H148Q containing additional single or double mutations.

libraries, respectively, and most of the colonies were fluorescent for the Leu201/Tyr203 library. Random sequencing of colonies revealed an excellent diversity of mutations.

An efficient screening protocol was developed to measure halide sensitivities of the expressed YFP mutants (Fig. 1). Bacterial strains and growth conditions were established to express YFPs in bacteria grown in 96-well microplates. After generation of replica 96-well microplates, bacteria were efficiently lysed in situ by digestion with lysozyme followed by repeated freeze-thaw. Bacterial debris after lysis remained on the bottom of the wells and so aliquots of the clear lysate could be transferred to secondary 96-well plates for halide titrations in a fluorescence plate reader.

Screening of 480 colonies from the Val150/Ile152 library gave YFP mutants with significantly different Cl^- and I^- affinities compared to YFP-H148Q, some of which are listed in Table 1. The I152L mutant had the lowest K_d for I^- (3 mM). Another mutant, V150A/I152L, was also strongly I^--sensitive (9 mM) but qualitatively less fluorescent. Screening of 672 colonies from the Val163/Phe165 library revealed two mutants with improved I^- sensitivity – V163A/F165Y ($K_d = 15$ mM) and V163T/F165Y ($K_d = 5$ mM), the latter being less fluorescent. Interestingly, mutant V163S had increased Cl^- sensitivity and decreased I^- sensitivity with respect to YFP-H148Q ($K_d = 62$ mM and 107 mM for Cl^- and I^-, respectively). Screening of the third library (384 colonies) revealed no mutants with improved halide sensitivities. Titrations with NO_3^- generally revealed K_d values intermediate to those for Cl^- and I^- (not shown), with the exception of I152L which had a K_d for NO_3^- (16 mM) that was much closer to that of I^-. Table 1 also shows that substantially lower Cl^- and I^- sensitivities were produced by introduction of hydrophilic amino acids at positions 150 and 163.

Three YFP mutants with potentially useful halide affinities for cellular applications (V150T, I152L and V163S) were purified (see inset Fig. 2) and analyzed further. Cl^-, I^- and NO_3^- titrations are shown in Fig. 2. Affinities for a series of anions are summarized in Table 2, along with nanosecond fluorescence lifetimes and molar extinction coefficients, quantum yields and kinetic analysis for the rates of Cl^- association and dissociation. Anion affinities determined here at pH 7.35 and constant ionic strength were slightly different from those in Table 1. The order of sensitivities to halides and nitrate were similar to that for YFP-H148Q except for V163S. Quantum yields were comparable, but molar extinction coefficients were somewhat lower for the mutants compared to YFP-H148Q. However, it should be noted that molar extinction coefficients were determined at pH 8.0 using the standardized method of Cubitt et al. [7] such that YFP variants with lower pK_a values will appear brighter than variants with higher pK_a values; after correction for pK_a, 'brightnesses' of the mutants and YFP-H148Q were comparable.

Further spectroscopic evaluation of YFP-H148Q mutant proteins is shown in Fig. 3. Peak excitation and emission wavelengths of the I152L mutant were 513 and 525 nm (Fig. 3A), similar to those of V150T and V163S (not shown). Nanosecond fluorescence lifetimes were similar for the mutants (Table 2), and not significantly altered by $[Cl^-]$ indicating a static quenching mechanism. The absorbance of each YFP-H148Q mutant was strongly affected by anion addition (e.g. NO_3^- effect on I152L, Fig. 3B), indicating that anions affect fluorescence by changing molar extinction coefficients.

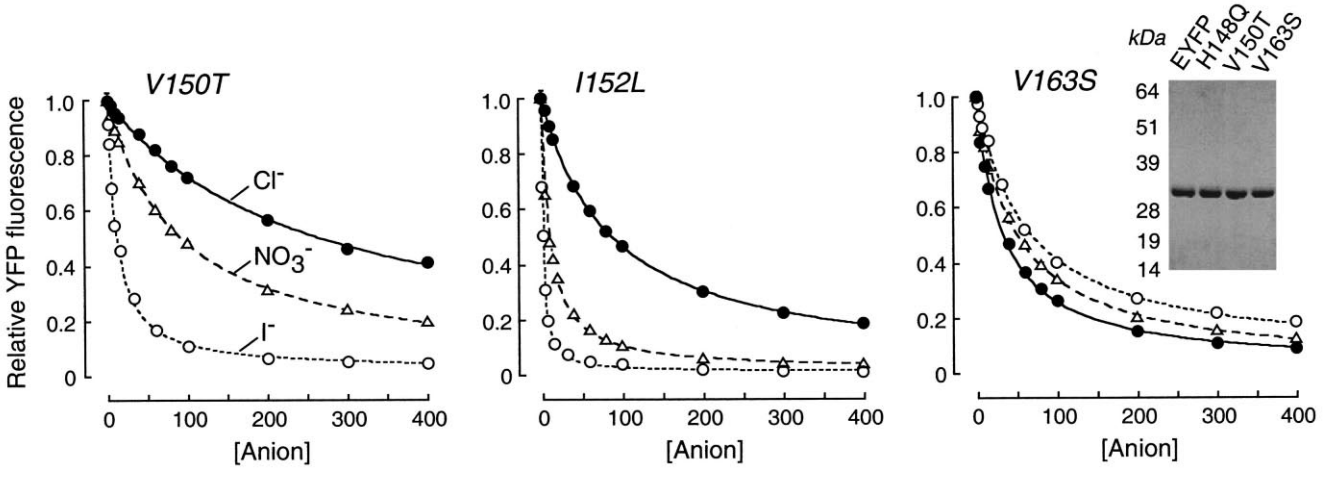

Fig. 2. Titrations of purified YFP-H148Q mutants V150T, I152L and V163S to Cl^-, I^- and NO_3^-. Titrations were carried out at pH 7.35 as described in Section 2. See Table 2 for fitted halide affinities. Inset: SDS–PAGE of purified YFP mutant proteins.

Table 2
Fluorescence properties of purified YFP mutants

	YFP-H148Q	YFP-H148Q V150T	YFP-H148Q I152L	YFP-H148Q V163S
Halide sensitivities and pK_a[a]				
K_{Cl} (mM)	106	258	85	39
K_{Br} (mM)	100	145	25	82
K_{NO_3} (mM)	36	91	10	51
K_I (mM)	11	11	1.9	62
K_F (mM)	2.7	10	2.3	0.85
pK_a	6.70	7.55	6.92	7.23
Fluorescence properties				
ε (M^{-1} cm^{-1})	71 000	43 500	52 200	45 300
Q_y	0.59	0.63	0.60	0.59
τ_f (ns)	3.1	2.9	2.8	3.4
YFP–chloride binding kinetics				
τ_{assoc} (ms)	286	190	54	1932
τ_{dissoc} (ms)	280	237	55	2138

[a]Halide affinities (K_X) and pK_a values of purified YFP-H148Q mutants were measured. Also shown are molar extinction coefficients (ε), quantum yields (Q_y) and nanosecond fluorescence lifetimes (τ_f), as well as exponential time constants for YFP–Cl^- association (τ_{assoc}) and dissociation (τ_{dissoc}). See text for explanations.

The absorption peaks at 513 nm and 410 nm correspond to the fluorescent deprotonated and non-fluorescent protonated forms of the chromophore, respectively. As found for YFP-H148Q [4], indicator pK_a decreased with increasing [Cl^-] (Fig. 3C); for I152L, the pK_a was 6.95 in the absence of Cl^-, increasing to 7.70 and 7.89 in the presence of 75 and 150 mM Cl^-, respectively. For V163S, the pK_a increased from 7.27 at 0 mM Cl^- to 7.97 at 75 mM Cl^-, and 8.18 at 150 mM Cl^- (data not shown). Fitted Hill coefficients (n_H) for all pH titrations were in the range 0.9–1.05. Cl^- binding and unbinding rates were comparable for YFP-H148Q and the V150T mutant (Fig. 3D, see Table 2 for exponential time constants), but substantially more rapid for I152L and slower for V163S. Together, these results suggest that fluorescence quenching of the YFP mutants occurs by static anion binding which results in a shift in pK_a and consequent decrease in absorbance.

The I152L mutant, which had the best I^- and NO_3^- sensitivities, was introduced into a mammalian expression vector to test its applicability to cellular anion exchange measurements. Transient transfection of Swiss 3T3 fibroblasts expressing CFTR gave cells that were brightly fluorescent with a

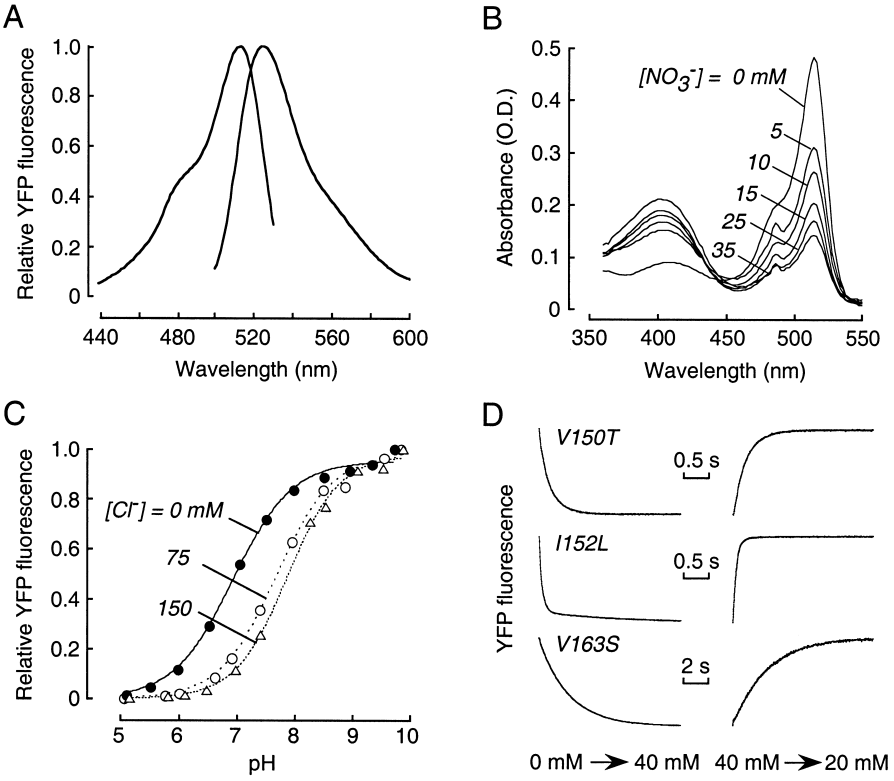

Fig. 3. Mechanistic analysis of anion binding to purified YFP-H148Q mutant proteins. A: Excitation and emission spectra of the I152L mutant. B: Absorbance spectrum of I152L at indicated [NO_3^-]. C: Fluorescence pH titrations of I152L done at indicated [Cl^-]. D: Cl^- association and dissociation kinetics of indicated YFP-H148Q mutants measured by stopped-flow fluorimetry. See text for explanations.

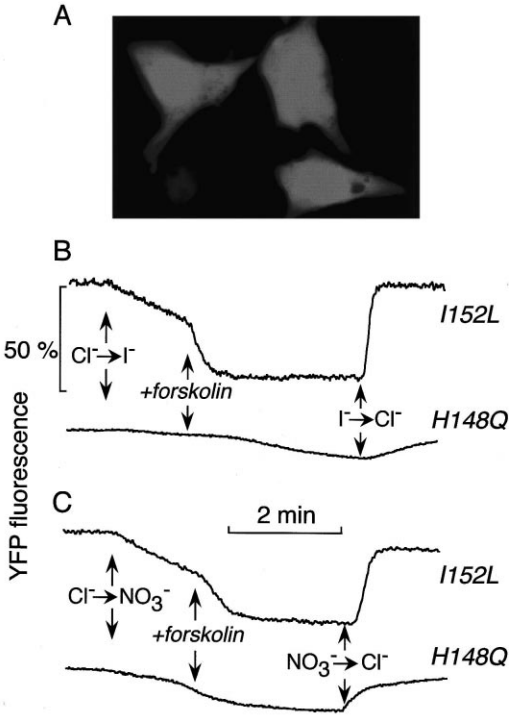

Fig. 4. CFTR-mediated halide transport in YFP-H148Q/I152L transfected CFTR-expressing 3T3 fibroblasts. A: Confocal fluorescence micrograph of transfected cells. B: Time course of fluorescence in response to exchange of 20 mM Cl^- for I^- and addition of forskolin. C: Time course in response to exchange of 100 mM Cl^- for NO_3^-. See text for explanations.

uniform cytoplasmic and nuclear staining pattern (Fig. 4A). Replacement of 20 mM Cl^- by I^- produced a slow decline in fluorescence due to basal CFTR activity, which increased rapidly with addition of the adenylate cyclase activator forskolin (Fig. 4B). The maximum fluorescence decrease of $53 \pm 2\%$ (S.E.M., $n = 4$) (upper curve) was much greater than that of $< 10\%$ for an identical experiment done with YFP-H148Q (lower curve). Last, given the significant sensitivity of I152L to NO_3^-, CFTR activity was also studied using a Cl^-/NO_3^- exchange protocol, which was again much less sensitive with YFP-H148Q (Fig. 4C). Replacement of 100 mM Cl^- by NO_3^- in I152L transfected cells showed a fluorescence decrease of $53 \pm 4\%$ ($n = 9$) (Fig. 4C).

4. Discussion

The motivation for the mutagenesis done here was the need for improved GFP-based halide indicators for cellular applications such as the measurement of intracellular Cl^- concentrations and cell membrane halide transport, particularly in the context of drug discovery by high-throughput screening. Screening of a focused set of YFP mutational libraries yielded indicators with different halide sensitivities and brightness, but with similar pK_a values and fluorescence spectra. Mutants with substantially improved I^- and NO_3^- sensitivities over YFP-H148Q were found, permitting the measurement of cellular halide transport by Cl^-/NO_3^- exchange or by Cl^-/I^- exchange using low I^- concentrations.

Analysis of the expressed mutated YFPs revealed a wide range of halide sensitivities, even with single amino acid substitutions, such as the replacement of isoleucine with leucine at residue 152. Many of the mutants had an I^- affinity greater than that of YFP-H148Q. The I152L and V150T mutants, as well as many of those listed in Table 1, have an anion selectivity sequence $I^- > NO_3^- > Br^- > Cl^-$, corresponding to a lyotropic sequence which is often found in halide binding proteins such as chloride channels [8,9]. This behavior suggests a weak field strength in the anion binding pocket. Accordingly, anions with lower dehydration energy such as I^- (283 vs. 347 kJ/mol for Cl^-, [9]) are favored. Although Cl^- has a smaller ionic radius than I^-, it is more strongly bound to adjacent water molecules and therefore less able to enter the protein pocket. The large increase in I^- affinity in I152L is probably due to a steric effect – a small change in cavity size may accommodate the large I^- anion much better.

An interesting finding was the identification of a YFP mutant, V163S, in which the sensitivity to Cl^- was greater than to I^-. The unusual selectivity sequence for V163S ($Cl^- > NO_3^- > I^- > Br^-$) may result from a more hydrophilic environment in the binding pocket. Interestingly, the relatively slow Cl^- binding and unbinding kinetics found in stopped-flow experiments suggest an increased energetic barrier, consistent with a conformational change in the anion binding cavity. Crystallographic information will be needed to resolve this issue. In terms of biological applications, the V163S mutant should permit the measurement of $[Cl^-]$ in organelles of the endosomal and secretory pathways, in which $[Cl^-]$ is predicted to be $\sim$25–40 mM, in the range of the Cl^- K_d of 39 mM of the V163S mutant but much lower than that of > 100 mM for YFP-H148Q. The challenge will be to correct $[Cl^-]$ for pH differences, which will require the generation of chimeric GFP-based indicators where $[Cl^-]$ and pH are measured in parallel.

A chimeric YFP-CFP (cyan fluorescent protein) was recently reported for monitoring intracellular changes in Cl^- associated with neuronal activity [10]. However, this probe has the limitation of very low Cl^- sensitivity. The YFP mutants identified here with greatly improved Cl^-, I^- and NO_3^- sensitivities will permit the design of sensitive dual-wavelength halide sensors for ratio imaging and cell cytometry applications.

Acknowledgements: We thank Dr. Sujatha Jayaraman for help in spectroscopic measurements and Ms. Karla Gregg for cell culture. Supported by Grants from the National Cystic Fibrosis Foundation, and the NIH (DK43840, HL60288, HL59198 and DK35124).

References

[1] Mansoura, M., Biwersi, J., Ashlock, M. and Verkman, A.S. (1999) Hum. Gene Ther. 10, 861–875.
[2] Jayaraman, S., Teitler, L., Skalski, B. and Verkman, A.S. (1999) Am. J. Physiol. 277, C1008–C1018.
[3] Wachter, R.M. and Remington, S.J. (1999) Curr. Biol. 9, R628–R629.
[4] Jayaraman, S., Haggie, P., Wachter, R.M., Remington, S.J. and Verkman, A.S. (2000) J. Biol. Chem. 275, 6047–6050.
[5] Wachter, R.M., Yarbough, D., Kallio, K. and Remington, S.J. (2000) J. Mol. Biol. 301, 157–171.
[6] Tsien, R.Y. (1998) Annu. Rev. Biochem. 67, 509–544.
[7] Cubitt, A.B., Woollenweber, L.A. and Heim, R. (1999) Methods Cell Biol. 58, 19–30.
[8] Wright, E.M. and Diamond, J.M. (1977) Physiol. Rev. 57, 109–156.
[9] Smith, S.S., Steinle, E.D., Meyerhoff, M.E. and Dawson, D.C. (1999) J. Gen. Physiol. 114, 799–817.
[10] Kuner, T. and Augustine, G.J. (2000) Neuron 27, 447–459.